Proceedings of the ASME 2013 International Design Engineering Technical Conferences & Computers and Information in Engineering Conference
IDETC/CIE 2013
August 4-7, 2013, Portland, Oregon, USA

DRAFT

DETC2013-13327

EXPERIMENTAL BLAST TESTING OF A LARGE 9-STORY STRUCTURE EQUIPPED WITH A SYSTEM OF NONLINEAR ENERGY SINKS

Nicholas E. Wierschem
Dept. of Civil and Environmental Engineering
University of Illinois
Urbana, IL, USA

Sean A. Hubbard
Dept. of Aerospace Engineering
University of Illinois
Urbana, IL, USA

Jie Luo
Dept. of Civil and Environmental Engineering
University of Illinois
Urbana, IL, USA

Larry A. Fahnestock
Dept. of Civil and Environmental Engineering
University of Illinois
Urbana, IL, USA

B. F. Spencer Jr.
Dept. of Civil and Environmental Engineering
University of Illinois
Urbana, IL, USA

D. Dane Quinn
Dept. of Mechanical Engineering
The University of Akron
Akron, OH, USA

D. Michael McFarland
Dept. of Aerospace Engineering
University of Illinois
Urbana, IL, USA

Alexander F. Vakakis
Dept. of Mechanical Science and Engineering
University of Illinois
Urbana, IL, USA

Lawrence A. Bergman
Dept. of Aerospace Engineering
University of Illinois
Urbana, IL, USA

ABSTRACT

In recent years the protection of structures from blasts has gained widespread attention with most of the effort on this subject focused on mitigating the local effects of the blast. With improved local protection, controlling the global response of structures subjected to impulsive types of loads is becoming increasingly important. In this paper, the passive mitigation of a structure's global response is examined through experimental blast tests of a large scale, 9-story structure equipped with a system of NESs. The system of NESs studied in this paper include two different types of devices, each of which employing a different type of restoring force; one type utilizes a smooth restoring force that is approximately cubic, while the other employs a linear restoring force coupled with one-sided vibro-impacts. The results of this study show that the passive NESs examined were capable of rapidly reducing the global response of the structure due to the blast loading. Additionally, the benefits of this passive system were demonstrated by its ability to reduce the peak demand on the structural system.

INTRODUCTION

During the past few decades, terrorist attacks, accidental explosions, and other blasts have critically affected building structures [1]. This vulnerability has spurred a large amount of research on the blast resistance of structures, with most of the recent efforts focused on local effects of the blast, progressive collapse, and resistance of nonstructural elements. Despite this recent focus, structures remain vulnerable to failure mechanisms related to their global response [2]. Furthermore,

 Copyright © 2013 by ASME

as the local protection of structures subjected to blast improves and failure mechanisms change, controlling a structure's global blast response is becoming increasingly important.

In recent years the ability of nonlinear energy sinks (NESs) to quickly mitigate the global response of structures subjected to impulsive loads has been extensively studied [3]–[8]. NESs are a type of passive mass damper; however, unlike traditional linear mass dampers, NESs utilize elements that produce an essentially nonlinear (non-linearizable) restoring force. With this essentially nonlinear restoring force, the response of an NES is not dominated by a single natural frequency and has the ability engage in resonant vibration with the primary structure across a broad frequency range. Thus, the NES can vibrate with any mode of an underlying structure and participate in Targeted Energy Transfer (TET) [9], the transfer of energy from lower modes of vibration to higher ones where it is can be dissipated more quickly. Furthermore, energy transferred to the NES itself can be dissipated by damping in the NES. Despite this research related to the mitigation of impulsive loads with NESs, most of this previous work uses only generalized impulsive loadings, and no experiments have been performed with a realistic blast.

In this paper, experimental blast testing of a large-scale structure equipped with a system of NESs is examined. The system of NESs which is used for blast protection in this study consists of a combination of two types of NESs. The first type of NES, known as a Type I NES, employs a smooth restoring force that is approximately cubic. The second type of NES, known as a single-sided vibro-impact NES (SSVI NES), utilizes a weak linear restoring force coupled with one-sided vibro-impacts. The results of this study show that the system of NESs examined is capable of rapidly mitigating the global response of the structure to a design blast load. Furthermore, this passive system of NESs is able to substantially reduce the peak demand on the system that results from this blast.

TEST STRUCTURE

The test structure used in this experimental study is shown in Figure 1. This structure, which was specifically developed for the large scale validation of a system of NESs, is 5.13 m tall and has a mass of approximately 11,000 kg. Currently, these dimensions make the structure the world's largest test bed for NES technology. Moreover, it is substantially larger in both height and mass than the previous largest test bed [10]. The structure consists of nine 2.74 m by 1.22 m steel plate floors and one 2.90 m by 1.22 steel base plate. The bottom 7 floors are solid 3.81 cm thick plate, while the base plate and the top two floors are 4.44 cm thick. Additionally, the two top floor plates have cutouts in them to accommodate the NESs within the floors. At the test site the structure is connected, via the base plate, to a concrete pad. The mass and dimensions of this pad are sufficient to ensure that during the blast testing the base of the structure is secured against movement.

Figure 1. Test Structure equipped with system of NESs

An identical column layout is used for each floor of the test structure. As shown in Figure 1, this layout consists of 8 columns that are arranged such that there is one bay in the short direction of the plates and 3 bays in the long direction. The columns are manufactured using high strength steel to allow the building to elastically accommodate relatively large deformations. All the columns in the structure are rectangular with the columns on bottom floor being 66.04 cm tall with a 19.05 cm by 1.43 cm cross-section. The columns used on every other floor are 50.80 cm tall and have a 13.97 cm by 1.43 cm cross-section. Because of their shapes, the bending stiffness of the columns in one direction is much larger than in the other. The columns are oriented so that their weak direction is along the short length of the plates and in the direction of the blast.

Covering one of the long sides of the test structure is the cladding. During the blast, the structure is positioned such that the cladded side is nearest to the blast. When the blast occurs, the pressure load that builds up on the cladding is transferred to the structure. The cladding is comprised of a series of overlapping 0.13 cm thick steel plates. The majority of these plates are 274 cm by 107 cm, which is long enough for the cladding sections to span between two floors. Two overlapped sections of cladding are connected to the structure via a row of 21 bolts into the side of the floor slab at floor levels 1 through 8. At these levels the overlapping cladding plates are also connected to each other via two rows of bolts above and below the floor plate connection. At the top of the structure, the 9th floor, one section of cladding is connected to the floor plate with a row bolts. Additionally, this top plate is also folded over and connected vertically to the plate with bolts. At the bottom of the structure one section of cladding is also attached

Copyright © 2013 by ASME

to the structure via a row of bolts. This bottom section of cladding is folded such that it is directly connected to the foundation via a row of anchors embedded into the concrete. Because of the relatively small mass of the cladding and its flexibility in the weak translational direction of the structure, its effect on the weak direction translational natural frequencies is minor. However, larger stiffness in torsion and strong translation mean that this cladding serves to increase, as compared with the structure without cladding, the torsional and strong direction translational natural frequencies.

During the initial phase of blast testing, some failure of the connection between the cladding and the structure occurred. For the subsequent tests the connection of the cladding was reinforced so that it could still transfer the pressure from the blast to the structure. No major effect on the modal properties of the structure resulted from this reinforcement.

To determine the modal parameters of the structure, instrumented hammer tests were performed. For this the NESs were locked, and the structure was considered to be linear. The results of testing identified natural frequencies of the structure in the weak direction of 1.74, 5.37, 9.10, 12.72, 15.96, 18.95, 21.63, 23.92, 25.48 Hz. Additionally, the torsional natural frequencies of the structure less than 30 Hz were determined to be 5.81, 18.16, and 29.36 Hz.

NONLINEAR ENERGY SINKS

As mentioned in the previous section, the NESs in the test structure are positioned within cutouts built into the floor plates of the 8th and 9th floors. These cutouts and NES masses, which are nearly identical for both floors, are shown in Figure 2. As this figure shows, three NESs are built into each of the top floors; the side two NESs are Type I NESs and the center is a single-sided vibro-impact NES (SSVI NES). Phenomenological models of these two types of NESs are shown in Figure 3. The idealized representations of both types of NESs are quite simple and consist of masses, springs, and dampers. The SSVI NES consists of a mass attached to a primary structure through a viscous damping element and a weak linear spring element; for this type of NES the relative displacement of the mass is limited on one side due to an impact surface that is connected to the primary structure. The result of these impacts is discontinuity in the restoring force. These discontinuities are broadband events and because of them energy is scattered throughout the structure, particularly to its higher modes [4]. Additionally, as shown in Figure 3, the Type I NES is composed of a mass connected to a primary structure through a viscous damping element and a smooth (no discontinuities in the restoring force) essentially nonlinear spring element. As a result of the smooth essential nonlinearity of this spring, the response of the NES is not dominated by a single natural frequency, and the device can resonate with and participate in the transfer of energy from any mode of the primary structure [3]. The transfer of energy to higher modes that occurs as a result of both types of NESs is beneficial because at these higher frequencies the energy can be naturally dissipated faster due to the reduced time scale. Furthermore, the damping elements in the NESs also help quickly eliminate the response of the test structure by dissipating energy when an NES moves relative to the floor it is located in.

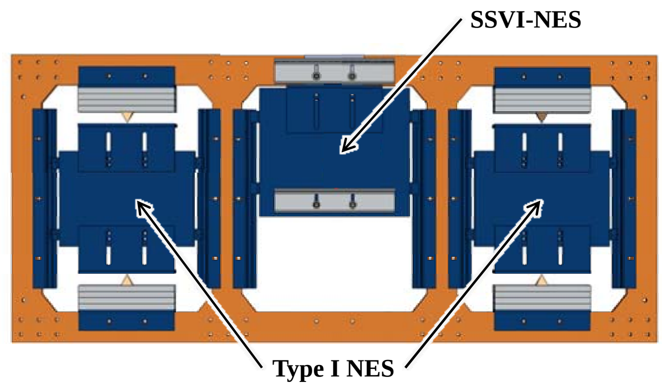

Figure 2. 8th and 9th Floors with built in NESs

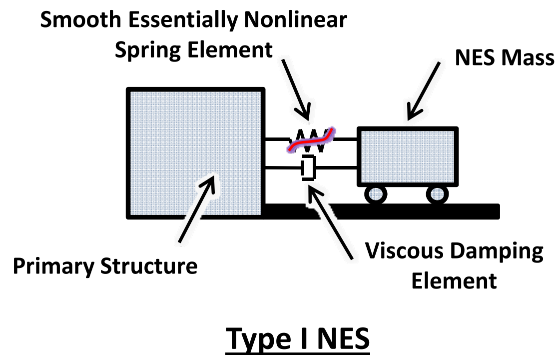

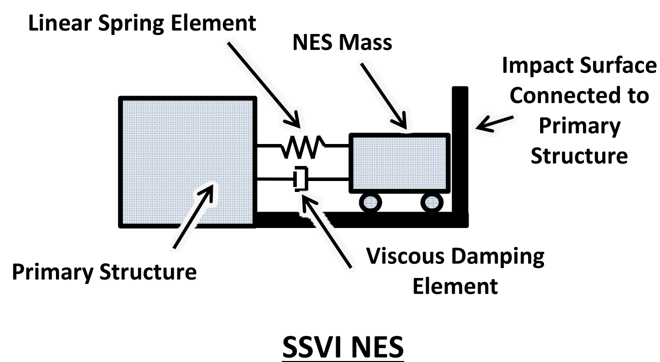

Figure 3: Phenomenological models of Type I and SSVI NESs

In the physical realization of these NESs, shown in Figure 2, all consist of solid steel masses that have Thomson

 Copyright © 2013 by ASME

SSUPB012 pillow blocks containing linear bearings mounted on their sides. These linear bearings allow the masses to move on sets of 1.91 cm round rail that are attached to the floor plate inside each cutout. The rails are positioned such that the masses move parallel to the short direction of the floor plate, in the direction of the blast. In the center of the 8^{th} and 9^{th} floors are SSVI NESs. Each SSVI-NES is coupled to the floor plate with a set of elastic cords. These elastic cords are positioned such that, at rest, the NES mass is in contact with one side of the floor plate. While unintended, there is a small amount of pretension in the elastic cords; the result of this is that the NES mass is secured against the side of the floor plate under very low loading conditions. When the motion of the floor is large enough to exceed this small pretensioning force the SSVI-NES moves relative to the floor. When this happens the elastic cords connecting the NES to the floor plate stretch and produce a restoring force that results in the NES mass being forced to collide with the floor with significant velocity. The result of this steel on steel collision is energy dissipation (the amount of which is related to the coefficient of restitution) and high frequency scattering of the remaining energy. The two NESs on each side of the floors shown in Figure 2 are the Type I NESs. These NESs are coupled to the structure using specially shaped elastomeric bumpers that are mounted on each side of the NES and are placed in compression when the NES moves. The special shape of these bumpers provides an essentially nonlinear, and approximately cubic, restoring force to the NES masses. Each Type I NES on the 8^{th} floor uses the same set of bumpers, but the Type I NESs on the 9^{th} floor use a different set. Each of the NESs in this system has its own locking mechanism; consequently, tests can be performed with the NESs locked (prevented from moving relative to the floor) or unlocked (free to move).

Using an estimate of the energy imparted to the structure from an idealized blast as a loading, the parameters of the NESs were determined through an optimization procedure. Here, the goal of the objective function was to maximize a measure of the apparent damping in the 1^{st} mode known as the effective damping [3]. The stiffness parameters for the NESs that resulted from this analysis, as well as the mass percentage of each NES, can be found in Table 1. These stiffness parameters were used to design the elastomeric bumpers for the Type I NESs and elastic cords for the SSVI NESs.

Table 1. Design values of mass and stiffness for NESs

	Mass (% of Structure Total Mass)	Design Stiffness Coefficient (N/m)	Design Stiffness Exponent
8th Floor Type I NES	1.5	7.56×10^8	3
9th Floor Type I NES	1.5	1.07×10^8	3
8th Floor SSVI NES	3.5	14546	1
9th Floor SSVI NES	3.5	12219	1

INSTRUMENTATION

A variety of instrumentation was utilized to record the loading and response of the structure during the blast testing, including accelerometers, pressure gages, strain gages, and displacement transducers. The accelerometers used for this testing were PCB model 353B33, Endevco model 7264-200, and Endevco model 7264-2000. The majority of these accelerometers were orientated to measure the response of the structure in the direction of the blast. Accordingly, accelerometers were placed on every floor of the structure and on each of the NESs. At locations of anticipated high acceleration, such as the SSVI NESs and the floors with NESs, the accelerometer models with higher maximum acceleration capacity were utilized. In addition to acceleration, direct measurements of the motions of the 1^{st} and 3^{rd} floors were obtained with displacement transducers.

To measure the demand on the 1^{st} story, several 1^{st} floor columns were instrumented with YEFLA-5-5LT strain gages manufactured by the Tokyo Sokki Kenkyujo Co. These gages were placed at mid-width of the columns and positioned 7.6 cm from the columns' end. This position allowed the strain gage to measure the strain resulting from the motion of the structure in the direction of the blast.

To measure the loading from the blast, the structure was instrumented with multiple pressure gages. These gages were attached to mounts directly connected to floor plates of the structure. So that it could measure the pressure on the face of the cladding, the head of the gage extended out of a small hole in the cladding.

BLAST LOADING DESIGN

Blast testing of the structure studied in this work was performed at the US Army Corps of Engineering Big Black Testing Range. This testing range is affiliated with and located near the US Army Corp of Engineering's Engineering Research

Copyright © 2013 by ASME

and Development Center in Vicksburg, Mississippi. Tests at this site were performed using air bursts of the high explosive C-4. For these tests the structure was orientated such that the structure's cladding faced towards the blast. With this orientation, the majority of the energy introduced into the structure from the blast resulted in the motion of the structure in its weak direction, as intended.

The objective of this testing was to evaluate the ability of the system of NESs to quickly eliminate the response of the structure due to a general blast loading. As a result of this objective, the goal of the charge designs was to provide a nearly uniform pressure impulse to the face of the cladding. When designing the charges for this testing the variables considered were the standoff distance (the horizontal distance of the charge from the structure), the height of the charge, and the weight of the charge. In general when the standoff distance is increased the uniformity of the pressure load on the structure also increases; however, with increased standoff distance, the pressure and resulting impulse on the structure is reduced. Consequently, if the standoff distance of a blast is increased, to maintain the same total average impulse on the structure the charge weight must also be increased.

Taking into account the variables of the charge configuration, the constraints on charge size due to the location of the test site, and the geometry of the test structure, the software UrbanFx, an extension of the BlastX software published by the US Army Corps of Engineering [12], was used to simulate the effects of the blast on the structure. With these simulations and a desired level of average pressure impulse, the charge configuration shown in Table 2 was designed. As seen from this table, the standoff distance of the blast is quite small. Because of limitation on charge size at the test site, this small standoff distance was necessary to provide the desired level of impulse.

Table 2. Charge configuration

Average Pressure Impulse (kPa-msec)	Standoff (cm)	Height of Burst (cm)	C-4 Charge Weight (kg)
209	213	295	1.40

In addition to calculating the average pressure impulse on the structure, the analysis with BlastFx provides the pressure impulse and maximum pressure at points along the structure's cladding face. Contour plots of the pressure impulse and maximum pressure on the structure for the blast listed in Table 2 are shown in Figure 4 and Figure 5, respectively. These contour plots show that, while the design goal of the blasts was to provide a uniform pressure impulse on the face of the structure, the resulting charge configurations deviate significantly from uniformity. Nonetheless, this charge configuration is adequate for this testing since, while not perfectly uniform, the pressure impulse is spread across the cladding.

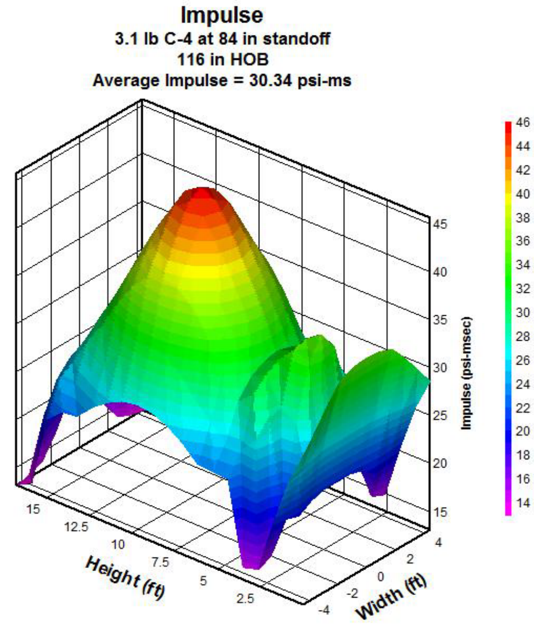

Figure 4. Cladding pressure impulse contour plot for design charge configuration

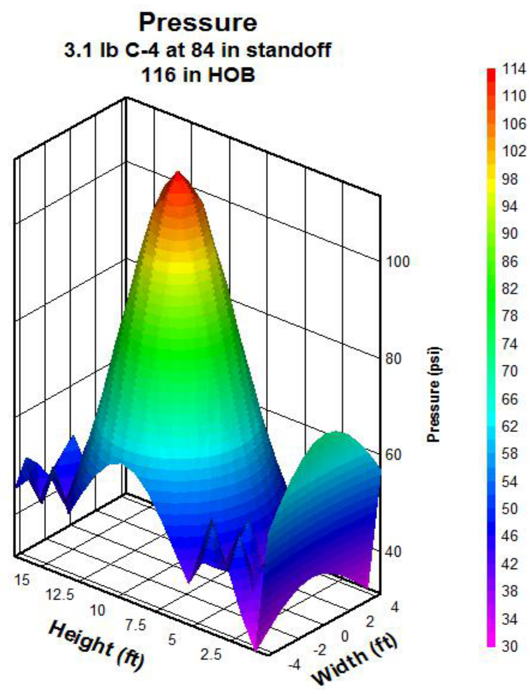

Figure 5. Maximum cladding pressure contour plot for design charge configuration

Copyright © 2013 by ASME

To produce the standoff distance and height of burst outline for the charge shown in Table 2, a system of rigging towers and cords was used to suspend the charges. Adjustable lengths of cord were attached to the charge and strung between two of the rigging towers to control the height of burst, while an additional cord attached to the charge and a third tower was used to control the standoff distance. The rigging towers, which can be partially seen in Figure 1, were constructed out of steel tubing, had a heavy base, and a small profile, which allowed them to survive the blast undamaged. The final component of the charge configuration, the weight of the charge, was simple to produce as the pliability of the C-4 made shaping into a sphere of exact weight easy.

EXPERIMENTAL RESULTS

Using the charge configuration outlined in Table 2 the structure was tested twice: first with the system of NESs unlocked (free to move) and then with the NESs locked (prevented from moving). In Figure 6 a frame from a high speed video of the blast during the 1st test is presented. As this frame was taken only milliseconds after the blast was initiated, the NESs, which are shown in the top two floors of the structure, have not yet had time to move significantly. What this frame does show is that the pressure wave resulting from the blast causes significant deformation to the cladding. Despite this deformation, after each test presented in this paper the cladding remained intact and, after slight repairs, was ready to transfer the load of the next blast to the structure.

Figure 6. Structure during blast testing

Pressure measurements taken from gages on the cladding during the test are shown in Figure 6, and the subsequent test with the NESs unlocked, are shown in Figure 7. The pressure gages used to obtain this figure are mounted on the 4th and 7th floors. As this figure shows, the gages on the 4th floor measure a much higher peak pressure than the ones on the 7th floor. Qualitatively, this result agrees with the simulation results found in Figure 5 and is logical as the gages on the 7th floor are further from the center of the blast than the 4th floor gages. Aside from differences in peak pressure, this figure also shows a time lag in the pressure measurements from the gages on separate floors. Once again, this is logical due to the proximity of the respective gages from the blast center. In addition to the characteristics of the blast pressure at different points along the cladding, Figure 7 demonstrates that the pressure loading on the structure for both tests is nearly equivalent, as the measurements from the NESs locked and unlocked tests show good agreement. This is important as it means the response of the structure from the two blasts can be accurately compared.

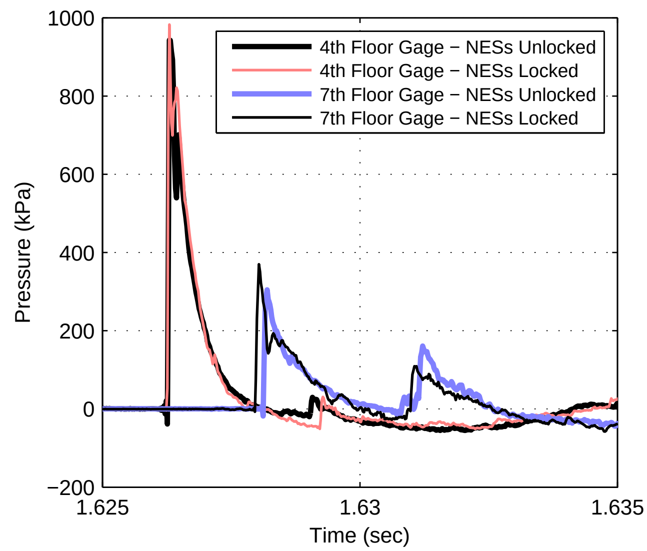

Figure 7. Pressure time history from various gages mounted in the center of the structure's width

In Figure 8 the 3rd floor displacement measured during the tests is shown. As this figure shows, when the NESs are unlocked the response of the structure rapidly decays; however, when the NESs are locked, the motion of the structure endures for a significantly longer time. Additionally, this figure shows that along with rapidly eliminating the motion, with the NESs unlocked the peak displacement at this floor level is reduced. The reduction observed in the positive direction is relatively small, but the reduction in the negative direction is quite substantial.

Copyright © 2013 by ASME

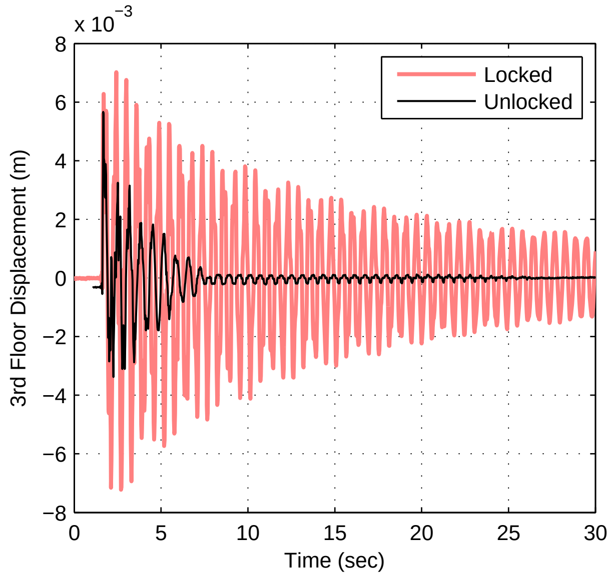

Figure 8. 3rd floor displacement response to blast

Figure 9 shows the wavelet spectra of the acceleration response of the 7th floor to the blast tests when the NESs are locked and unlocked. The wavelet spectrum can be a useful tool for examining the behavior of the structure because it is capable of showing changes in the frequency content of the structure's response over time [13]. As Figure 9 shows, when the NESs are locked the 7th floor acceleration response of the structure due to the blast is spread over most of the modes of the structure in the weak translational direction; however, the most significant, and prolonged, motion is observed in the lowest three modes. When the NESs are unlocked Figure 9 shows that motion in nearly all the modes of the structure decay faster than the case when the NESs are locked; this is especially true for the lowest modes of the structure which decay very rapidly when the NESs are unlocked. Furthermore, as the input from the blasts was comparable for the two tests, this figure suggests the transfer of energy to the higher modes of the structure due to motion of the NESs as these wavelet spectra show greater emphasis in higher modes of the structure's response when the NESs are unlocked.

To better understand the behavior shown in Figure 9, Figure 10 shows the time history and wavelet spectra of the acceleration response of the 8th floor NESs during the blast test when they are unlocked. This figure shows that the NESs undergo large accelerations, but are only in motion for a few seconds after the blast. During this time the frequency content of the response of the NESs is very broadband, as expected due to the essential nonlinearities in the restoring force the NESs are designed with. This broadband behavior is especially apparent during the impacts of the SSVI, which correspond with the peaks in the time history of the SSVI NES's acceleration and the matching dark bands in the wavelet spectra. This broadband behavior of the NESs is what allows them to couple the modes of the structure and engage in targeted energy transfer.

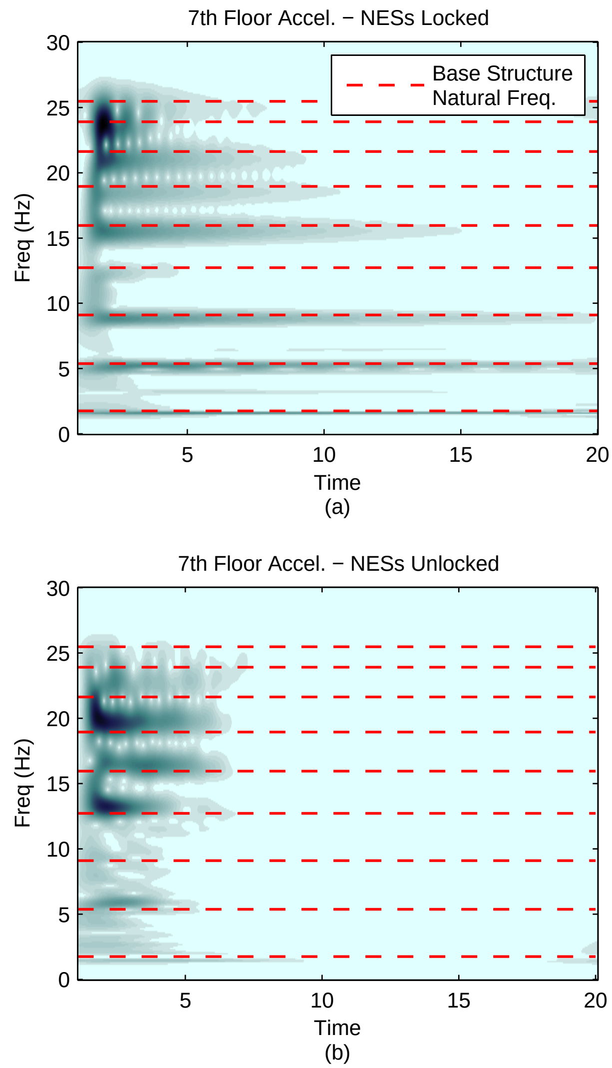

Figure 9. Wavelet spectra of the 7th floor acceleration with (a) NES locked (b) NESs unlocked

Copyright © 2013 by ASME

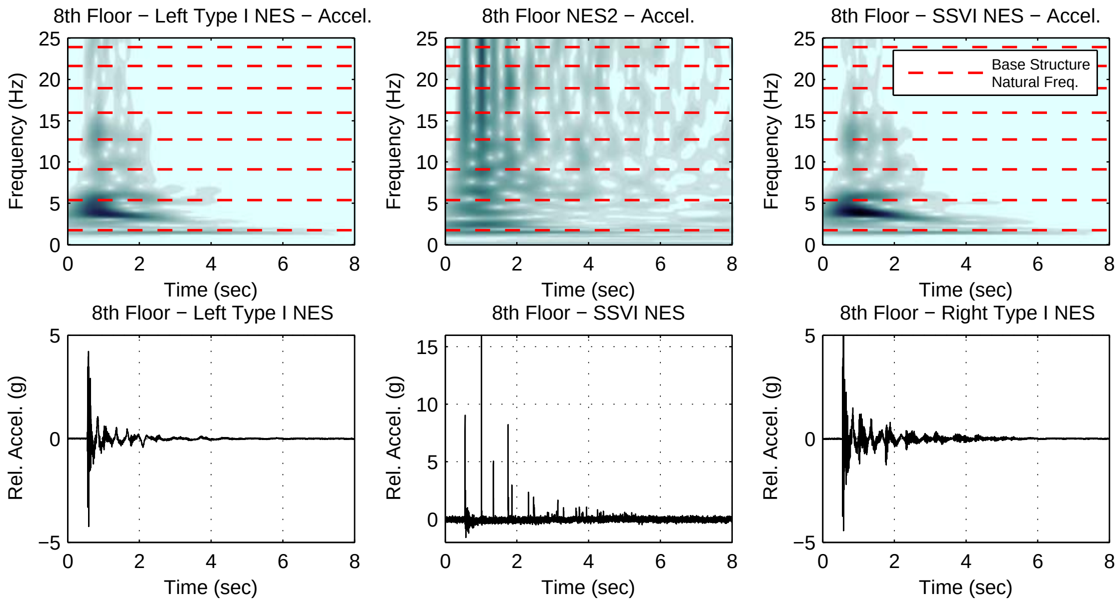

Figure 10. 8th Floor NESs Acceleration response - time history and wavelet spectra

Examining the resulting displacements and accelerations from the blast loading is useful for investigating the behavior of the structure; however, these measures do not directly correspond with the demand on the structure. To examine the demand on the structure, the strain measured at one of the interior 1st floor columns is shown in Figure 11. This strain is proportional to the column moment which results from the blast loading; thus, this measurement can be used examine the structural demands on the 1st story, which is often times the most critical part of a structure. Figure 11 shows that, like the displacement and acceleration responses previously examined, the strain in the 1st floor columns decays quickly when the NESs are unlocked. Additionally, with a reduction of 21.9% in measured strain compared to the locked case, this figure demonstrates that the passive system of NESs is able to substantially reduce the maximum demand on the 1st floor due to the blast.

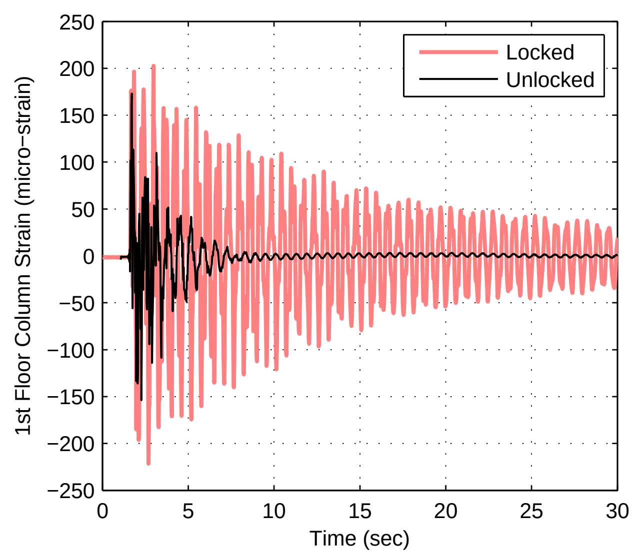

Figure 11. 1st floor column strain response to blast

CONCLUSION

In this paper the experimental blast testing of a large scale 9-story structure equipped with a system of nonlinear energy sinks (NESs) was examined. The system includes two different types of NESs. One type utilizes a smooth restoring force that is approximately cubic and realized with specially shaped elastomeric bumpers, while the other NES utilizes a weakly linear restoring force coupled with one-sided vibro-impacts. The results of this testing show that the system of NESs is able to quickly diminish the global response of the structure due to

Copyright © 2013 by ASME

the blast loading. This rapid reduction of response corresponds with broadband motion of the NESs and significant transfer of energy from the lower modes of the structure to its higher modes. Additionally, comparisons with blast tests when the system of NESs was locked show that the passive system of NESs studied in this paper is capable of reducing peak demand on the structure, as measured by the strain in the 1st floor columns.

ACKNOWLEDGMENTS

This research program is sponsored by the Defense Advanced Research Projects Agency through grant HR0011–10–1–0077; Dr. Aaron Lazarus is the program manager. The content of this paper does not necessarily reflect the position or the policy of the Government, and no official endorsement should be inferred.

REFERENCES

[1] C. L. Elliott, G. C. Mays, and P. D. Smith, "The protection of buildings against terrorism and disorder," *Proceedings of the ICE - Structures and Buildings*, vol. 94, pp. 287–297, 1992.

[2] T. Ngo, P. Mendis, A. Gupta, and J. Ramsay, "Blast loading and blast effects on structures–An overview," *Electronic Journal of Structural Engineering*, vol. 7, pp. 76–91, 2007.

[3] T. P. Sapsis, D. D. Quinn, A. F. Vakakis, and L. A. Bergman, "Effective Stiffening and Damping Enhancement of Structures With Strongly Nonlinear Local Attachments," *J. Vib. Acoust.*, vol. 134, no. 1, pp. 011016–12, Feb. 2012.

[4] M. A. Al-Shudeifat, N. E. Wierschem, D. D. Quinn, A. F. Vakakis, L. A. Bergman, and B. F. Spencer Jr., "Numerical and Experimental Investigation of a Highly Effective Single-Sided Vibro-Impact Nonlinear Energy Sink for Shock Mitigation," *International Journal of Non-Linear Mechanics*, accepted for publication.

[5] N. E. Wierschem, D. D. Quinn, S. A. Hubbard, M. A. Al-Shudeifat, D. M. McFarland, J. Luo, L. A. Fahnestock, B. F. Spencer Jr., A. F. Vakakis, and L. A. Bergman, "Passive Damping Enhancement of a Two-degree-of-freedom System Through a Strongly Nonlinear Two-degree-of-freedom Attachment," *Journal of Sound and Vibration*, vol. 331, pp. 5393–5407, 2012.

[6] D. Dane Quinn, Angela L. Triplett, Alexander F. Vakakis, and Alexander F. Vakakis, "Energy Harvesting From Impulsive Loads Using Intentional Essential Nonlinearities."

[7] B. Vaurigaud, A. T. Savadkoohi, and C.-H. Lamarque, "Efficient Targeted Energy Transfer With Parallel Nonlinear Energy Sinks: Theory and Experiments," *Journal of Computational and Nonlinear Dynamics*, vol. 6, no. 4, p. 041005, 2011.

[8] F. Schmidt and C. H. Lamarque, "Energy pumping for mechanical systems involving non-smooth Saint-Venant terms," *International Journal of Non-Linear Mechanics*, vol. 45, no. 9, pp. 866–875, 2010.

[9] G. Kerschen, A. F. Vakakis, Y. S. Lee, D. M. McFarland, and L. A. Bergman, "Toward a Fundamental Understanding of the Hilbert-Huang Transform in Nonlinear Structural Dynamics," *Journal of Vibration and Control*, vol. 14, no. 1–2, pp. 77 –105, Jan. 2008.

[10] N. E. Wierschem, J. Luo, M. A. Al-Shudeifat, S. A. Hubbard, R. J. Ott, L. A. Fahnestock, D. M. McFarland, B. F. Spencer Jr., A. F. Vakakis, and L. A. Bergman, "Simulation and Testing of a 6-Story Structure Incorporating a coupled two Mass Nonlinear Energy Sink," in *Proceedings of the ASME 2012 International Design Engineering Technical Conferences & Computers and Information in Engineering Conference*, Chicago, USA, 2012.

[11] D. M. Boore and J. J. Bommer, "Processing of strong-motion accelerograms: needs, options and consequences," *Soil Dynamics and Earthquake Engineering*, vol. 25, no. 2, pp. 93–115, 2005.

[12] J. R. Britt, D. E. Ranta, and C. E. Joachim, *BlastX code, version 4.2, user's manual*. Vicksburg, MS: U.S. Army Engineering Research and Development Center.

[13] D. Labat, "Recent advances in wavelet analyses: Part 1. A review of concepts," *Journal of Hydrology*, vol. 314, no. 1–4, pp. 275–288, 2005.

 Copyright © 2013 by ASME